Polymer Journal (2016) 48, 875–881

www.nature.com/pj

ORIGINAL ARTICLE

Assembly structure and rod orientation of rod–coil diblock copolymer films

Ya-Juan Su, Ze-Xin Ma and Jian-Hua Huang

The self-assembly and rod orientation of rod–coil (RC) diblock copolymer (DBC) films confined between two identical impenetrable and rod-selective walls was investigated by performing dissipative particle dynamics simulations. Various structures, such as a wetting layer near the surfaces, perpendicular cylinders, parallel cylinders and island-like structures, were observed. Thus a morphological phase diagram as a function of the film thickness and rod length was presented. A long-range rod–rod orientational order was observed in the assembly structures for a rod block above a critical rod length. The critical rod length for the disorder–order transition of the rod orientation was found to be dependent on the assembly structure and film thickness. Our results indicate that the rod length and film thickness influence both the assembly structure and the rod orientation of RC DBCs.
Polymer Journal (2016) **48,** 875–881; doi:10.1038/pj.2016.47; published online 18 May 2016

INTRODUCTION

Diblock copolymer (DBC) thin films are highly relevant to several industrial applications because they are able to self-assemble into ordered domains of controllable shapes at a nanometer scale. Significant efforts using both experimental and theoretical studies have been devoted to understanding and controlling the self-assembly of DBCs.[1,2] In addition to the segregation strength and the fraction of the individual blocks, two additional factors, that is, the polymer–surface interaction and the film thickness, have significant roles in the self-assembly of DBCs in thin films. Therefore, various morphologies deviating from the bulk structure have been observed in the films.[1–4] For rod–coil (RC) DBCs, the difference in the chain conformational entropy between the rod and the coil blocks and the liquid crystal behavior of the rod blocks as well as the effects of the confinement on the orientation of rod blocks result in more complex structures than that of coil–coil (CC) DBCs.[5–10]

Rich structures of the RC DBCs in films were observed in experiments in addition to normal parallel lamellae ($L_{\parallel}$) and perpendicular lamellae ($L_{\perp}$). For instance, poly(alkoxyphenylenevinylene-*b*-isoprene) (PPV-*b*-PI) RC DBCs formed islands and holes when the film thickness did not match the natural domain spacing of the RC DBCs.[7] Poly(2,5-dioctyloxy-p-phenylene vinylene)-b-polystyrene (PS) RC DBCs formed highly ordered honeycomb structures.[11] Radzilowski and Stupp[12] observed that the RC DBCs changed from alternating strips to a hexagonal superlattice of rod aggregates in the film with a decrease in the fraction of the rod block. Chen and Thomas[13] reported the zigzag morphology assembled by poly(*n*-hexyl isocyanate)-b-PS RC DBCs in thin films. These experimental results implied that the assembly structures of the RC DBCs were dependent on several factors, such as the composition of the copolymer and the property of the film surface. However, the mechanism for the self-assembly of the RC DBCs in film is not clear. Conversely, it was determined to be quite difficult to obtain equilibrium assembly structures of RC DBCs in thin films in experiments because they could form aggregates or micelles, and the structures were often kinetically trapped in the film.[7,14] Therefore, theoretical studies and computer simulations are important tools to understand the equilibrium assembly structures of RC DBCs confined in thin films.

The rich assembly structures could be understood as that smectic RC DBC melts confined between two flat surfaces are considerably more constrained than the analogous CC DBC system.[15] Islands and holes in the RC DBC films resulted from the incommensurability between the film thickness and the natural domain spacing of the DBCs.[7] Therefore, $L_{\perp}$ was expected to form in relatively thick films.[15] Using extended scaling methods, Nowak and Vilgis[16] concluded that when the RC DBCs were adsorbed on the surface, the rod blocks tended to arrange parallel to the surface to gain entropy and lower their confinement energy. Using a self-consistent field theory calculation, Yang *et al.*[14] determined that the rod block indicated a strong tendency to segregate near the surfaces in all structures owing to its smaller conformational entropy loss compared with the coil block. In our previous report, we investigated the self-assembly of lamella-forming RC DBCs within a rod-selective slit based on dissipative particle dynamics (DPD) simulations.[17] The self-assembled structure was found to be sensitively dependent on the rigidity and fraction of the rod block and the slit thickness. Several ordered structures, such as hexagonally packed cylinders perpendicular to the surfaces, $L_{\perp}$ and $L_{\parallel}$, were assembled.[17] Furthermore, DFT calculations were performed to explore the effects of the chain rigidity and surface property on the assembly structures.[18] These studies indicated that semi-flexible copolymers under confinement behave differently than flexible copolymers.

Department of Chemistry, Zhejiang Sci-Tech University, Hangzhou Xiasha Higher Educational Zone, Hangzhou, China
Correspondence: Professor J-H Huang, Department of Chemistry, Zhejiang Sci-Tech University, Hangzhou Xiasha Higher Educational Zone, Hangzhou 310018, China.
E-mail: jhhuang@zstu.edu.cn
Received 16 January 2016; revised 13 March 2016; accepted 15 March 2016; published online 18 May 2016

Based on their composition, RC DBCs can form various structures in bulk, such as separated aggregates, cylinders and lamellae.[19] RC DBCs with a small volume fraction of the rod block form separated aggregates in bulk. Most simulation studies on confined RC DBCs have focused on the lamella-forming RC DBCs, whereas less attention was given to the aggregate-forming RC DBC systems either from experiments or simulations. Additionally, it is more difficult to imagine the results in detail for aggregate-forming systems confined in film. In the current study, we performed DPD simulations to study the self-assembly of aggregate-forming RC DBC films confined between two identical impenetrable and rod-selective walls. The effects of the rod length in the RC DBC and the film thickness on the assembled structure and rod orientation were systematically investigated.

MATERIALS AND METHODS

DPD algorithm

The DPD method was developed by Hoogerbrugge and Koelman[20] and cast in its current form by Español.[21] In the DPD simulations, fluid elements are coarsely grained into the DPD particles. These DPD particles interact with each other via pairwise forces that locally conserve momentum, resulting in a correct hydrodynamic description.[22] The pairwise forces contain the conservative force $\mathbf{F}_{ij}^{(C)} = a_{ij}w(r_{ij})\hat{\mathbf{r}}_{ij}$, dissipative force $\mathbf{F}_{ij}^{(D)} = -\gamma w^2(r_{ij})(\hat{\mathbf{r}}_{ij}\cdot\mathbf{v}_{ij})\hat{\mathbf{r}}_{ij}$ and random force $\mathbf{F}_{ij}^{(R)} = \sigma w(r_{ij})\theta_{ij}\hat{\mathbf{r}}_{ij}$, where $r_{ij}=|\mathbf{r}_{ij}|=|\mathbf{r}_i-\mathbf{r}_j|$; $\hat{\mathbf{r}}_{ij}=\mathbf{r}_{ij}/r_{ij}$; $\mathbf{v}_{ij}=\mathbf{v}_i-\mathbf{v}_j$; θ_{ij} is an uncorrelated symmetric random noise with zero mean and unit variance; σ is the amplitude of the thermal noise; and γ is a friction coefficient. The combined effect of the dissipative and random forces is similar to that of a thermostat, resulting in $\sigma^2=2\gamma k_BT$, where k_B is the Boltzmann constant and T is the temperature. The softness of the interaction is determined by the weight function $w(r_{ij})$ with a commonly used selection: $w(r_{ij})=1-r_{ij}/r_c$ for $r_{ij}\leqslant r_c$ and $w(r_{ij})=0$ for $r_{ij}>r_c$, where r_c is the cutoff radius. The interaction parameter a_{ij} is the strength of the repulsive interaction dependent on the species of particles i and j. The values of a_{ij} will be presented subsequently.

In our DPD simulations, all of the DPD particles are of the same mass with $m=1$. We set the cutoff distance $r_c=1$ as the unit of length and $k_BT=1$ as the scale of energy. Thus the unit of force is k_BT/r_c and that of time is $\tau=\sqrt{mr_c^2/k_BT}$. In this study, the amplitude of random noise is set at $\sigma=3$.

The DPD particles move according to Newton's equation. The position and velocity of the particles are solved using a modified Velocity–Verlet algorithm with a time step of $\Delta t=0.01$.[23]

Model of the RC DBC film

The RC DBC film is considered to be confined between two identical impenetrable parallel walls along the z direction. Each wall with a thickness of $1r_c$ is constructed by four layers of DPD particles that are arranged in a face-centered cubic lattice. The film thickness H varies from 4 to 20 in the current study. Periodic boundary conditions are applied in the x and y directions. For simplicity, the wall DPD particles are motionless in the simulations.

The RC DBC is modeled as a coarse-grained linear chain $R_{N_R}C_{N_C}$ with N_R DPD particles in the rod (R) block and N_C DPD particles in the coil (C) block. A finitely extensible non-linear elastic (FENE) interaction is used for the chemically bonded monomers. The bonded FENE interaction U_{FENE} can be represented as follows:[24]

$$U_{i,i+1}^{FENE}=\begin{cases}-\frac{k_F}{2}(r_{max}-r_{eq})^2\ln\left[1-\left(\frac{r_{i,i+1}-r_{eq}}{r_{max}-r_{eq}}\right)^2\right] & \text{for } 2r_{eq}-r_{max}<r_{i,i+1}<r_{max},\\ \infty & \text{otherwise}\end{cases} \quad (1)$$

where the equilibrium bond length $r_{eq}=0.8$; maximum bond length $r_{max}=1.3$; and elastic coefficient $k_F=40$. For the rod block, an additional bending energy between the consecutive bonds can be introduced as follows[25]:

$$U_{bend}=\frac{1}{2}k_\theta(\theta-\theta_0)^2 \quad (2)$$

where k_θ and $\theta_0=\pi$ are the bending modulus and the equilibrium angle between two consecutive bonds, respectively. Specifically, $k_\theta=0$ corresponds to a flexible block, similar to the coil block in the present model. The rigidity of the rod block increases with an increase in k_θ. In this study, we select a relatively large value of $k_\theta=50$. The average bond angle $<\theta>$ in the rod block is approximately 170°, thus indicating that the rod block is quite rigid.

The overall particle density is set at three throughout this study. In our system, there are three species of the DPD particles: R and C monomers in the copolymer chain, and wall particles (W). The repulsive interaction parameter between identical species is set at 25, that is, $a_{RR}=a_{CC}=a_{WW}=25$. A slightly large $a_{RC}=32.9$ is selected between the R and C monomers to ensure the formation of an aggregate phase in bulk for the R_5C_{13} DBCs.[19] The wall surface is assumed to have a rod-preference, with $a_{WR}=5$ and $a_{WC}=25$.

The assembly structures presented in this report are the equilibrium structures obtained after a sufficiently long simulation time. The total simulation time for each independent run is approximately 10^5 DPD time units. Polymer chains are generated randomly in the system at the beginning of the simulation. We check the evolution of the structure as well as the system energy. The system is assumed to reach equilibrium state when both the structure and the system energy fluctuate with time for at least 5×10^4 DPD time units.

RESULTS AND DISCUSSION

First, we simulated the structure of the RC DBCs in bulk. The interaction parameter between the rod and the coil blocks was set at $a_{RC}=32.9$. Figure 1 depicts a typical equilibrium structure formed by the R_5C_{13} DBCs in a $30\times30\times30$ box with periodic boundary conditions in all three directions. It can be clearly seen that the R-rich domains form separated aggregates embathed inside the C-rich matrix, which is in agreement with the theoretical prediction based on the SCF lattice model.[19] Similar structures were observed for different independent simulation runs.

Then we investigated the self-assembly of the R_5C_{13} DBC films confined between two rod-selective walls. The effects of the film thickness H on the assembled morphology was investigated by varying H from 4 to 20 with a step of 2. Moreover, the dependence of the assembled structure and the rod orientation on the rod length N_R was further studied. Previous investigations indicated that the rod length

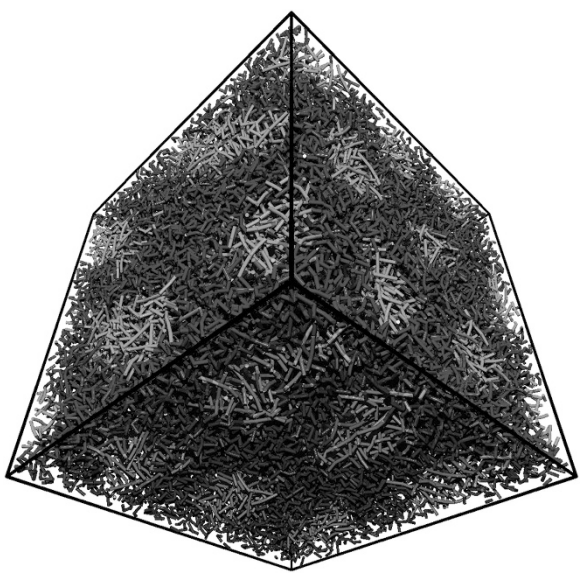

Figure 1 Equilibrium structure assembled by the R_5C_{13} DBCs in bulk. The R blocks are represented in red, whereas the C blocks are represented in blue. The same colors are used in the remaining figures. A full color version of this figure is available at the *Polymer Journal* online.

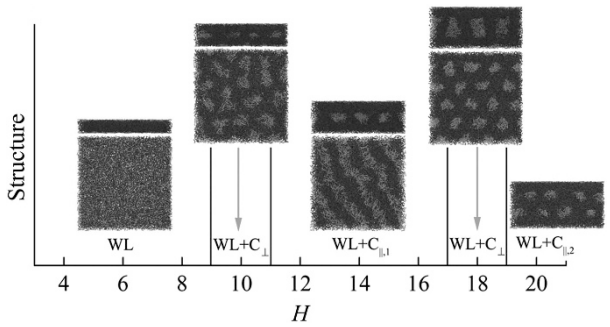

Figure 2 Equilibrium structures of the R_5C_{13} DBC films confined between two rod-selective walls with $a_{WR}=5$ and $a_{WC}=25$. For the WL, the side view (top) and the top view (bottom) are presented. For WL+$C_\perp$ and WL+$C_{||,1}$, the side view (top) and the top view at the center (bottom) of the system are presented. Only the side view is depicted for the structure formed at $H=20$. For clarity, the wall particles are not shown in all figures. A full color version of this figure is available at the *Polymer Journal* online.

was a primary factor that led to the disorder–order transition in RC copolymer systems, and the coil length had a secondary effect on the orientational order of the rod blocks.[26,27] Thus we studied the effects of the rod length by varying N_R from 5 to 9 with the volume fraction of the R block f_R maintained at approximately 0.28. For a few typical structures, the effects of $N_R=10$ were also calculated. We determined that the assembly structure of the RC DBCs was sensitively dependent on the film thickness and the rod length.

Simulations were performed in systems with a lateral size $L_x=L_y$. The effects of the lateral size on the assembly structure were investigated. We determined that the assembly structures were nearly independent of the lateral size when it reached 40 for $N_R\leqslant 8$. However, $L_x=L_y=50$ was sufficiently large for $N_R=9$ and 10. For each set of parameters, at least 10 independent samples were used in the simulations. Furthermore, we determined that the results were sample independent.

Assembly of the R_5C_{13} DBC films confined between two rod-selective walls

When the R_5C_{13} DBCs were confined between rod-selective walls with $a_{WR}=5$ and $a_{WC}=25$, various structures were observed with a change in the film thickness H. Typical structures at $H=6$, 10, 14, 18 and 20 are presented in Figure 2. In thin films with $H<10$, the rod blocks formed a wetting layer (WL) near the wall surfaces. In fact, the WL of the rod blocks was always observed in all films. With an increase in H, new structures were formed at the center of the film. Furthermore, the structure at the center of the film was dependent on the film thickness H. When H was increased to 10, perpendicular cylinders ($C_\perp$) were formed by the rod blocks at the center of the film. Additionally, one-layer parallel cylinders ($C_{||,1}$) were assembled by the rod blocks for H ranging from 11 to 17. However, when H reached 18, the $C_\perp$ structure was formed again. Afterwards, two-layer parallel cylinders ($C_{||,2}$) were assembled by the rod blocks at $H=20$. In our simulations, a mixed structure of parallel and perpendicular cylinders was not observed. It appears that the assembly structure is dependent on the slit thickness. In short, the rod blocks displayed a series of WL-WL+$C_\perp$-WL+$C_{||,1}$-WL+$C_\perp$-WL+$C_{||,2}$ with an increase in H. The results indicate that the film thickness has an important role in the formation of ordered structures for the R_5C_{13} copolymers.

The appearance of the WL can be attributed to the energy favor of the rod blocks. Additionally, the formation of cylinders can be attributed to the different properties of the rod and coil blocks. However, the driving force for the parallel and perpendicular cylinders in slits may be the competition between the slit thickness and cylinder diameter.

A similar morphological variation with an increase in H was observed when a_{WR} was varied from 5 to 25 while maintaining $a_{WC}=25$, where $a_{WR}=25$ is the limitation of the rod-selective wall. The results indicate that the assembly structure is roughly independent of the interaction parameter a_{WR}. In fact, the wall surface is not rod-selective at $a_{WR}=25$. The formation of the WL at $a_{WR}=25$ is due to the strong conformational asymmetry between the rod and coil blocks. The coil blocks lose significantly more conformational entropy near an impenetrable surface than the rigid rods and are thus depleted from the surface. Therefore, an energetically neutral and impenetrable surface exhibits an entropic preference for the rod blocks.[14] This result is closely related to the phenomenon in experiments in which the rod layers are particularly well developed near the film surface.[28]

The appearance of cylinders is consistent with the theoretical prediction that a sphere-to-cylinder transition will occur under an external field (strain, electric field, confinement).[29–31] Furthermore, the WL structure was reported in the sphere-forming PS-b-poly (ethylene-alt-propylene) film.[32]

Additionally, the assembly structures of the RC DBCs are different from that of the CC DBCs. Brennan's group[33] reported a series of $C_\perp$-WL-WL+$C_{||,1}$-WL+$PL_{||,1}$-WL+$C_{||,1}$-WL+$C_{||,2}$-WL+$PL_{||,2}$ when increasing the slit thickness for flexible A_3B_7 DBCs within an A-selective slit, where $PL_{||,\nu}$ represents a parallel perforated lamellar phase with ν periodic layers. Tan *et al.*[30,31] studied the morphologies of sphere-forming flexible A_8B_2 copolymers confined between two homogeneous surfaces. A series of morphologies, including spheres, WL, $C_\perp$, $C_{||}$, perforated lamellae and lamellae, were obtained by varying the slit thickness and the surface field strength.[30,31] Similar morphologies were assembled by the confined A_6B_3 DBCs.[34] A thin film system of asymmetric A_9B_{27} DBCs was studied using MC simulations by Wang *et al.*[35] In addition to $C_\perp$ and $C_{||}$, they observed one layer of spheres between two A WLs for the A-preferential surfaces.[35] Our results indicate that the rod block in the DBC has a special role in the formation of the assembly structure for the DBCs.

Effects of the rod length

It is known that a rod block in RC copolymers can affect the self-assembly behavior, including aggregation morphology and disorder–order transition.[26,36,37] Pryamitsyn and Ganesan[36] indicated that the effects of the rod block were more evident for longer rod blocks, and there was a critical rod length of approximately 8–9 that induced the disorder–order transition.

In this subsection, we studied the effects of the rod length on the assembly structure and rod orientation by changing N_R from 5 to 9 while keeping $f_R\approx 0.28$. In the simulations, $a_{RC}=32.9$ and $k_\theta=50$ were kept as constants. The wall surface was still considered to be rod-selective with $a_{WR}=5$ and $a_{WC}=25$, and the film thickness H was varied from 4 to 20.

For RC DBC thin films with $H\leqslant 8$, R blocks formed a WL near surfaces independent of the rod length N_R; however, the degree of rod alignment in the WL definitely depended on N_R. As an example, Figures 3a and b depict the equilibrium structures of the R_6C_{15} and R_9C_{23} DBCs formed at $H=6$, respectively. It is clear that the orientational order of the rod blocks for the R_9C_{23} DBCs within the WL was considerably better than that of the R_6C_{15} DBCs. For the R_9C_{23} DBCs, the rod blocks tended to be parallel to each other.

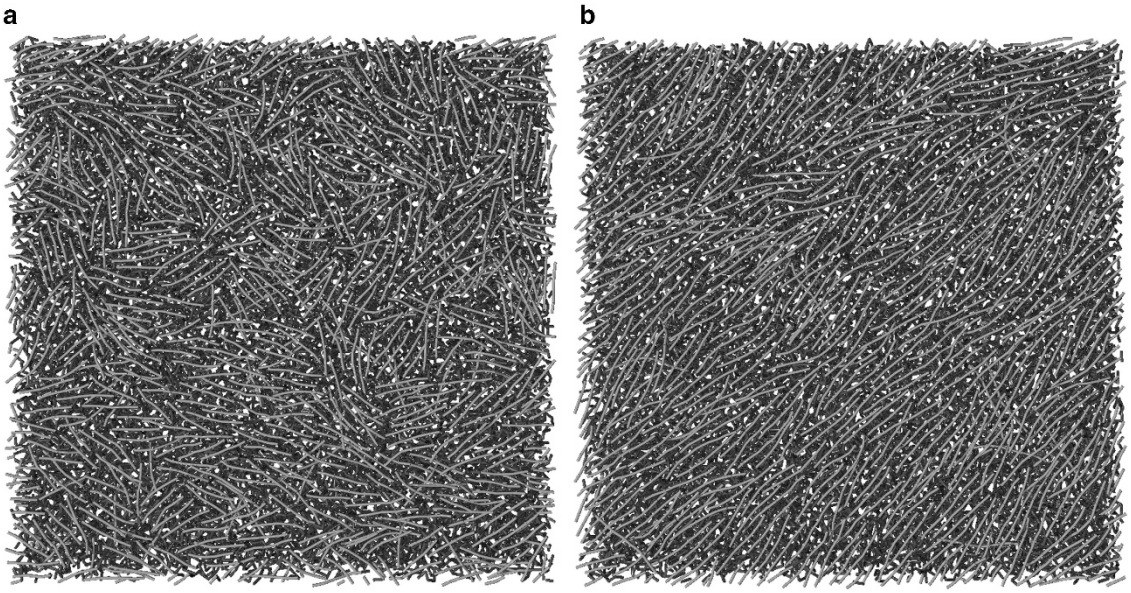

Figure 3 Top view of the equilibrium structure for R_6C_{15} (**a**) and R_9C_{23} (**b**) DBC films formed at $H=6$. A full color version of this figure is available at the *Polymer Journal* online.

To quantify the alignment of the rod blocks within the WL, a rod–rod orientational order parameter was calculated for the rod blocks. We can define the rod–rod orientational order parameter as follows:

$$s(r)=\frac{\sum_{i<j}\left(\frac{3\cos^2\theta_{ij}-1}{2}\right)\delta(r-r_{ij})f(\vec{r}_i,\vec{r}_j)}{\sum_{i<j}\delta(r-r_{ij})f(\vec{r}_i,\vec{r}_j)}, \quad (3)$$

which is similar to that defined in Chou *et al.*[26]. Here θ_{ij} is the included angle between two rods; and r_{ij} is the distance between the mass centers of rod *i* and rod *j*. A sketch for θ_{ij}, and r_{ij} is presented in Figure 4. The delta function can be defined as follows:

$$\delta(x)=\begin{cases}1, & 0<x<1\\ 0, & \text{otherwise}\end{cases}. \quad (4)$$

Additionally, we can introduce a condition function $f(\vec{r}_i,\vec{r}_j)$ for calculating the orientational order parameter. For WL, $f(\vec{r}_i,\vec{r}_j)=1$ when both rods are in the same WL, otherwise $f(\vec{r}_i,\vec{r}_j)=0$. Thus $s(r)$ is calculated in each WL and further averaged over two WLs near the upper and lower surfaces.

Here the rod–rod orientational order parameter $s(r)$ represents the space correlation between the rod blocks. Thus $s=0$ for a completely random and isotropic sample, whereas $s=1$ for a perfectly aligned sample.[26]

The dependence of $s(r)$ on the rod–rod distance r for the various $R_{N_R}C_{N_C}$ DBCs in the WL is presented in Figure 5a. For $N_R<7$, the order parameter was small and decayed rapidly with distance, thus indicating that the rods were roughly randomly oriented in a long length scale. However, for $N_R>7$, s was large and decayed slowly with distance, thus indicating an ordered arrangement for the rod blocks. It was noted that, for a typical liquid crystal sample, s was on the order of 0.3–0.8.[26] Our results indicate that there is a long-range orientation order for $N_R>7$ and a short-range order for $N_R<7$. The existence of a short-range orientation order for the rod length $N_R<7$ is clearly different from that of similar copolymers in solution.[26] Therefore, the simulation results indicate that the confinement helps establish a short-range orientation order for the rod blocks. In Figure 5b, we present the mean orientational order parameter $<s>$ for different rod lengths N_R. Here $<s>$ is averaged over all rod–rod pairs in the WLs. We determined that $<s>$ clearly increased from $N_R=7$.

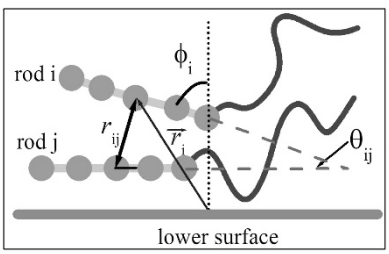

Figure 4 Sketch of two RC copolymers, rod *i* and rod *j*, near the surface. Here θ_{ij} and r_{ij} is the included angle between the two rods and the distance between the mass centers of rod *i* and rod *j*, respectively. Additionally, $\vec{r}_i$ is the position vector of the mass center of rod *i*, and ϕ_i is the angle between the rod *i* and the surface normal direction. A full color version of this figure is available at the *Polymer Journal* online.

Our results indicate that there is a critical rod length $N_R^*=7$ for the disorder–order transition of the rod orientation in the WL structure. N_R^* was observed to be dependent of the assembly structure and condition.[27] For instance, $N_R^*=9$ was estimated for the RC copolymers in solution.[26] It was noted that the rod length was a primary factor that led to the disorder–order transition in RC copolymer systems.[26,27] Our results indicate that the confinement may also have a role in the disorder–order transition in copolymer films.

The orientation of the rod blocks in the WL was further analyzed by the angle ϕ_i between the rod *i* and the surface normal direction, as sketched in Figure 4. We determined that the mean angle $<\phi>$ in Figure 5c was close to 90° for all of the RC DBCs, thus indicating that the rod blocks were nearly parallel to the surfaces. Although the rod blocks were parallel to the surface, the space correlation between the

rod blocks demonstrated different behaviors for short rods ($N_R<7$) and long rods ($N_R>7$), as presented in Figure 5a. Nevertheless, a short-range orientation order existed for all $R_{N_R}C_{N_C}$ DBCs with either a short or long rod block.

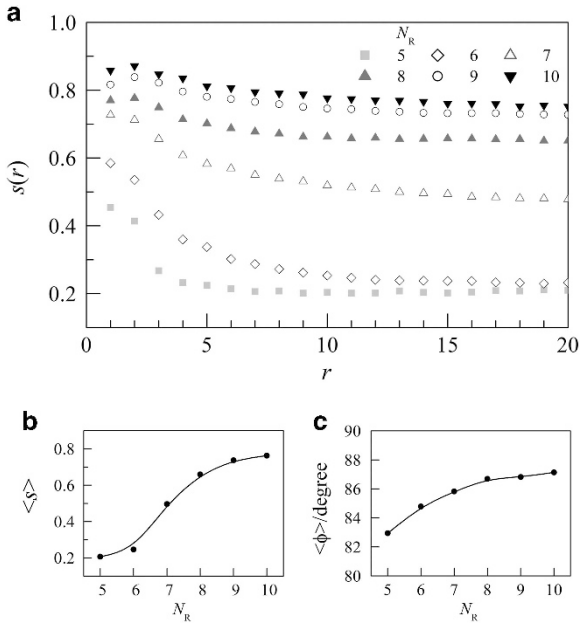

Figure 5 (**a**) Rod–rod orientational order parameter $s(r)$; (**b**) mean orientational order parameter $<s>$; and (**c**) mean angle $<\phi>$ of the rod blocks in the WL for different $R_{N_R}C_{N_C}$ DBC films with $H=6$. A full color version of this figure is available at the *Polymer Journal* online.

We determined that the structure is dependent on the rod length when the film thickness is >8. For example, the equilibrium structures formed by the R_6C_{15} and R_9C_{23} DBCs at $H=10$ are presented in Figures 6a and b, respectively. These structures were clearly different from that of $N_R=5$, where WL+$C_\perp$ was formed by the rod blocks, as shown in Figure 2. Instead, an island-like (I) structure was assembled by the rod blocks at $N_R=6$ and 7, and parallel half-cylinders ($C_{||,1/2}$) of the rod blocks near the surfaces were assembled by the rod blocks for $N_R=8$ and 9. It was assumed that a small degree of orientational freedom may stabilize the semi-cylindrical structure.[27]

Figure 7 illustrates the phase diagram of the $R_{N_R}C_{N_C}$ copolymers in terms of the rod length N_R and the film thickness H. Here N_R was varied from 5 to 9 while H was varied from 4 to 20. The film thickness is in the unit of the size of the DPD bead. There is a simple relation between H and N_R because the physical length of the rod is approximately $(N_R-1)r_{eq}$ with $r_{eq}=0.8$. We observed five assembly structures: WL, I, WL+$C_\perp$, WL+$C_{||,1}$, WL+$C_{||,2}$, and $C_{||,1/2}$. In fact, a rod layer near the surface (known as WL) with a depth of approximately $1r_c$ was always observed. Generally, the RC DBCs form a WL in thin films and a WL+$C_{||}$ in thick films. However, the structures in moderately thick films are strongly dependent on the rod length.

It is easy for RC DBCs to form a WL near the surfaces and a $C_{||}$ structure in the interior region of the thick films, as indicated in Figure 7. As an example, we calculated the rod–rod orientational order parameter $s(r)$ in these two structures at $H=16$. In the $C_{||,1}$ structure, $s(r)$ was calculated for each single cylinder and then averaged over all of the cylinders. Figure 8a presents $s(r)$ in the WL and $C_{||,1}$ for the R_8C_{21} and $R_{10}C_{26}$ DBCs. The mean orientational order parameter $<s>$ for the different rod lengths N_R in the WL and $C_{||,1}$ are plotted in

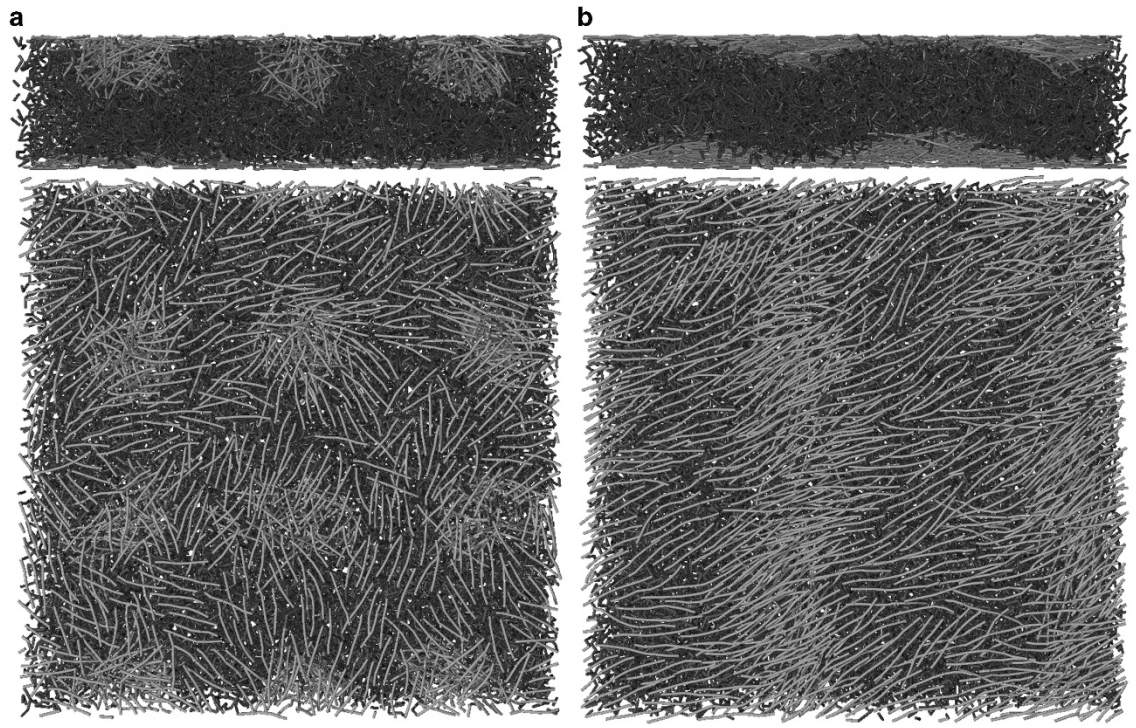

Figure 6 Top view (top) and side view (bottom) of the equilibrium structure assembled by the R_6C_{15} (**a**) and R_9C_{23} (**b**) DBC films with $H=10$. A full color version of this figure is available at the *Polymer Journal* online.

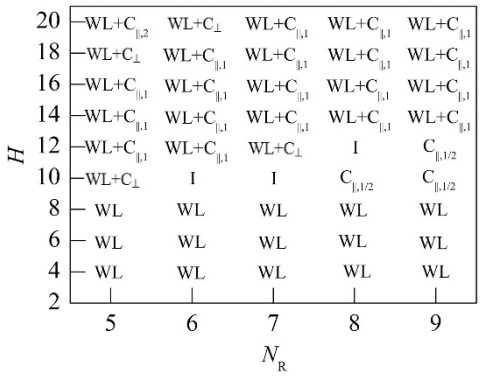

Figure 7 Dependence of the morphologies of the $R_{N_R}C_{N_C}$ DBCs on the rod length N_R and the film thickness H confined between two rod-selective walls with $a_{WR}=5$ and $a_{WC}=25$. The depicted structures are the wetting layer (WL), wetting layer and perpendicular cylinders (WL+$C_{\perp}$), wetting layer and one-layer parallel cylinders (WL+$C_{\parallel,1}$), wetting layer and two-layer parallel cylinders (WL+$C_{\parallel,2}$), island-like structure (I) and parallel half-cylindrical structure ($C_{\parallel,1/2}$).

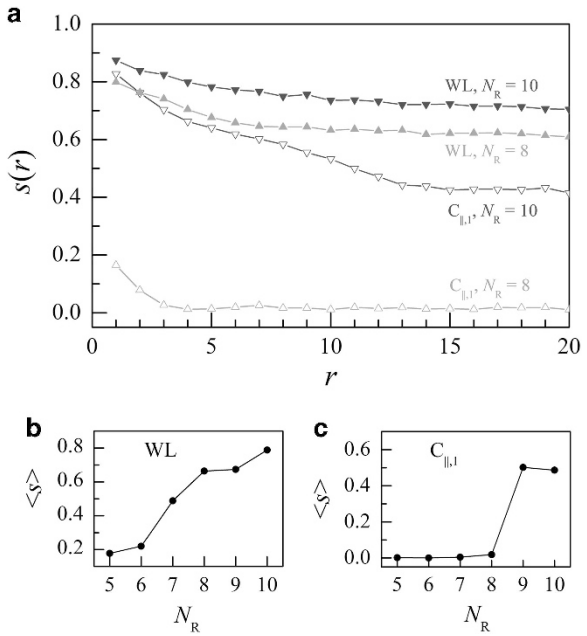

Figure 8 (**a**) Rod–rod orientational order parameter $s(r)$ of the rod blocks in the WL and $C_{\parallel,1}$ for the R_8C_{21} and $R_{10}C_{26}$ DBC films. The dependence of the mean orientational order parameter $<s>$ on the rod length N_R in (**b**) WL and (**c**) $C_{\parallel,1}$ for $H=16$. A full color version of this figure is available at the *Polymer Journal* online.

Figures 8b and c, respectively. We determined that $s(r)$ in the WL at $H=16$ is approximately the same as that in the WL of the thin film with $H=6$, as indicated in Figure 5a. Furthermore, the disorder–order transition occurs at $N_R^*=7$, as seen in Figure 8b. Additionally, we can determine that $s(r)$ in the WL is larger than that in the $C_{\parallel,1}$ structure, thus indicating that the rod blocks in WL are more ordered than those in $C_{\parallel,1}$. Particularly, for the R_8C_{21} DBCs, the rod blocks are ordered in the WL, whereas they are randomly oriented in the $C_{\parallel,1}$ structure. The critical rod length is $N_R^*=9$ for the $C_{\parallel,1}$ structure (Figure 8c), which is the same as that of the RC copolymers in solution.[26] Our results indicate that a critical rod length N_R^* for the disorder–order transition of the rod orientation can always be found in the RC DBC systems. However, for the assembly structure near the surface, N_R^* is smaller, whereas $s(r)$ is larger. This result implies that the rod orientation in the RC DBC films is different from that in the solution. Furthermore, the confinement effect of the surfaces on the RC DBCs exists near the surfaces but fades in the interior region away from the surfaces at a large H.

CONCLUSION

In this study, the self-assembly of $R_{N_R}C_{N_C}$ DBC films confined between two rod-selective walls was examined by performing dissipative particle dynamics simulations. The RC copolymers with a small rod fraction of $f_R\approx0.28$ formed separated aggregates in bulk and different assembly structures in films. The effects of the film thickness H and the rod length N_R on the self-assembly of the confined RC DBCs and the rod–rod orientation of the rod blocks were systematically investigated. Thus a morphological phase diagram of the assembly structures as a function of H and N_R was presented. The results indicated that WL and WL+$C_{\parallel}$ were generally formed in thin and thick films, respectively, and the structures were nearly independent of the rod length. However, in moderately thick films, different morphologies, such as an island-like structure and a parallel half-cylindrical structure, were observed for a variation in the rod length.

For a typical WL formed in thin films ($H=6$) and WL+$C_{\parallel,1}$ in thick films ($H=16$), the rod–rod orientational order parameter of the rod blocks was calculated. The orientations of the rod blocks in both WL structures were similar. It was determined that the rod blocks tended to orient parallel to each other when the rod length exceeded a critical rod length. The critical rod length for the disorder–order transition of the rod orientation was determined to be dependent on the assembly structure. We found that the orientational order of the rod blocks in the WL was better than that in the $C_{\parallel,1}$, and the critical rod length for the WL was smaller than that for the $C_{\parallel,1}$.

Our simulation results indicate that the film thickness and the rod length influence both the assembly structure and the rod orientation of RC DBC. Furthermore, confinement can significantly influence the rod orientation of RC DBCs near surfaces.

CONFLICT OF INTEREST

The authors declare no conflict of interest.

ACKNOWLEDGEMENTS

This study was supported by the National Natural Science Foundation of China (21574117).

1 Knoll, A., Horvat, A., Lyakhova, K. S., Krausch, G., Sevink, G. J. A., Zvelindovsky, A. V. & Magerle, R. Phase behavior in thin films of cylinder-forming block copolymers. *Phys. Rev. Lett.* **89**, 035501 (2002).
2 Nikoubashman, A., Register, A. & Panagiotopoulos, A. Z. Self-assembly of cylinder-forming diblock copolymer thin films. *Macromolecules* **46**, 6651–6658 (2013).
3 Darling, S. B. Directing the self-assembly of block copolymers. *Prog. Polym. Sci.* **32**, 1152–1204 (2007).
4 Hamley, I. W. Ordering in thin films of block copolymers: fundamentals to potential applications. *Prog. Polym. Sci.* **34**, 1161–1210 (2009).
5 Radzilowski, L. H., Carragher, B. O. & Stupp, S. I. Three-dimensional self-assembly of rodcoil copolymer nanostructures. *Macromolecules* **30**, 2110–2119 (1997).
6 Lin, S. L., He, X. H., Li, Y. L., Lin, J. P. & Nose, T. Brownian molecular dynamics simulation on self-assembly behavior of diblock copolymers: influence of chain conformation. *J. Phys. Chem. B* **113**, 13926–13934 (2009).
7 Olsen, B. D., Li, X. F., Wang, J. & Segalman, R. A. Thin film structure of symmetric rod-coil block copolymers. *Macromolecules* **40**, 3287–3295 (2007).
8 Wang, Q. Theory and simulation of the self-assembly of rod-coil block copolymer melts: recent progress. *Soft Matter* **7**, 3711–3716 (2011).

9 Braun, C. H., Schöpf, B., Ngov, C., Brochon, C., Hadziioannou, G., Crossland, E. J. W. & Ludwigs, S. Synthesis and thin film phase behavior of functional rod-coil block copolymers based on poly(para-phenylenevinylene) and poly(lactic acid). *Macromol. Rapid Commun.* **32**, 813–819 (2011).
10 Park, J. W. & Cho, Y. H. Surface-induced morphologies in thin films of a rod-coil diblock copolymer. *Langmuir* **22**, 10898–10903 (2006).
11 de Boer, B., Stalmach, U., Nijland, H. & Hadziioannou, G. Microporous honeycomb-structured films of semiconducting block copolymers and their use as patterned templates. *Adv. Mater.* **12**, 1581–1583 (2000).
12 Radzilowski, L. H. & Stupp, S. I. Nanophase separation in monodisperse rodcoil diblock polymers. *Macromolecules* **27**, 7747–7753 (1994).
13 Chen, J. T. & Thomas, E. L. The use of force modulation microscopy to investigate block copolymer morphology. *J. Mater. Sci.* **31**, 2531–2538 (1996).
14 Yang, G., Tang, P., Yang, Y. L. & Wang, Q. Self-assembled microstructures of confined rod-coil diblock copolymers by self-consistent field theory. *J. Phys. Chem. B* **114**, 14897–14906 (2010).
15 Pereira, G. G. & Williams, D. R. M. Smectic rod-coil melts confined between flat plates: monolayer-bilayer and parallel-perpendicular transitions. *Macromolecules* **33**, 3166–3172 (2000).
16 Nowak, C. & Vilgis, T. A. Aggregates of rod-coil diblock copolymers adsorbed at a surface. *J. Chem. Phys.* **124**, 234909 (2006).
17 Huang, J. H., Ma, Z. X. & Luo, M. B. Self-assembly of rod-coil diblock copolymers within a rod-selective slit: a dissipative particle dynamics simulation study. *Langmuir* **30**, 6267–6273 (2014).
18 Turesson, M., Forsman, J. & Åkesson, T. Simulations and density functional calculations of surface forces in the presence of semiflexible polymers. *Phys. Rev. E* **76**, 021801 (2007).
19 Chen, J. Z., Zhang, C. X., Sun, Z. Y., Zheng, Y. S. & An, L. J. A novel self-consistent-field lattice model for block copolymers. *J. Chem. Phys.* **124**, 104907 (2006).
20 Hoogerbrugge, P. J. & Koelman, J. M. V. A. Simulating microscopic hydrodynamic phenomena with dissipative particle dynamics. *Europhys. Lett.* **19**, 155–160 (1992).
21 Español, P. Dissipative particle dynamics with energy conservation. *Europhys. Lett.* **40**, 631–636 (1997).
22 Ripoll, M., Ernst, M. H. & Español, P. Large scale and mesoscopic hydrodynamics for dissipative particle dynamics. *J. Chem. Phys.* **115**, 7271–7284 (2001).
23 Groot, R. D. & Warren, P. B. Dissipative particle dynamics: Bridging the gap between atomistic and mesoscopic simulation. *J. Chem. Phys.* **107**, 4423–4435 (1997).
24 Kremer, K. & Grest, G. S. Dynamics of entangled linear polymer melts-a molecular-dynamics simulation. *J. Chem. Phys.* **92**, 5057–5086 (1990).
25 AlSunaidi, A., den Otter, W. K. & Clarke, J. H. R. Liquid-crystalline ordering in rod-coil diblock copolymers studied by mesoscale simulations. *Philos. Trans. R. Soc. Lond. A* **362**, 1773–1781 (2004).
26 Chou, S. H., Tsao, H. K. & Sheng, Y. J. Structural aggregates of rod-coil copolymer solutions. *J. Chem. Phys.* **134**, 034904 (2011).
27 Horsch, M. A., Zhang, Z. L. & Glotzer, S. C. Self-assembly of end-tethered nanorods in a neat system and role of block fractions and aspect ratio. *Soft Matter* **6**, 945–954 (2010).
28 Park, J. W. & Thomas, E. L. Multiple ordering transitions: Hierarchical self-assembly of rod-coil block copolymers. *Adv. Mater.* **15**, 585–588 (2003).
29 Pereira, G. G. Cubic to cylindrical transition in diblock copolymers induced by strain. *Macromolecules* **37**, 1611–1620 (2004).
30 Tan, H. G., Yan, D. D. & Shi, A. C. Surface effect on the body-centered-cubic phase of diblock copolymers. *Macromolecules* **37**, 9646–9653 (2004).
31 Tan, H. G., Song, Q. G., Yang, S., Yan, D. D. & Shi, A. C. Confinement effect on the body-centered-cubic phase of diblock copolymers in film. *Macromol. Theory Simul.* **17**, 45–51 (2008).
32 Lawrence, N. T., Kehoe, J. M., Hoffman, D. B., Marks, C., Yarbrough, J. M., Atkinson, G. M., Register, R. A., Fasolka, M. J. & Trawick, M. L. Combinatorial mapping of substrate step edge effects on diblock copolymer thin film morphology and orientation. *Macromol. Rapid Commun.* **31**, 1003–1009 (2010).
33 Petrus, P., Lísal, M. & Brennan, J. K. Self-assembly of lamellar- and cylinder-forming diblock copolymers in planar slits: insight from dissipative particle dynamics simulations. *Langmuir* **26**, 14680–14693 (2010).
34 Huinink, H. P., van Dijk, M. A., Brokken-Zijp, J. C. M. & Sevink, G. J. A. Surface-induced transitions in thin films of asymmetric diblock copolymers. *Macromolecules* **34**, 5325–5330 (2001).
35 Wang, Q., Nealey, P. F. & de Pablo, J. J. Monte Carlo simulations of asymmetric diblock copolymer thin films confined between two homogeneous surfaces. *Macromolecules* **34**, 3458–3470 (2001).
36 Pryamitsyn, V. & Ganesan, V. Self-assembly of rod-coil block copolymers. *J. Chem. Phys.* **120**, 5824–5838 (2004).
37 Fan, Z. X., Ma, Z. X. & Huang, J. H. Dissipative particle dynamics simulations on self-assembly of rod-coil-rod triblock copolymers in a rod-selective solvent. *J. Chem. Phys.* **139**, 064905 (2013).